

IQGAP1, a Rac- and Cdc42-binding Protein, Directly Binds and Cross-links Microfilaments

Anne-Marie Bashour,* Aaron T. Fullerton,* Matthew J. Hart,[‡] and George S. Bloom*

*Department of Cell Biology and Neuroscience, University of Texas Southwestern Medical Center, Dallas, Texas 75235; and

[‡]Onyx Pharmaceuticals, Richmond, California 94806

Abstract. Activated forms of the GTPases, Rac and Cdc42, are known to stimulate formation of microfilament-rich lamellipodia and filopodia, respectively, but the underlying mechanisms have remained obscure. We now report the purification and characterization of a protein, IQGAP1, which is likely to mediate effects of these GTPases on microfilaments. Native IQGAP1 purified from bovine adrenal comprises two ~190-kD subunits per molecule plus substoichiometric calmodulin. Purified IQGAP1 bound directly to F-actin and cross-linked the actin filaments into irregular, interconnected bundles that exhibited gel-like properties. Exog-

enous calmodulin partially inhibited binding of IQGAP1 to F-actin, and was more effective in the absence, than in the presence of calcium. Immunofluorescence microscopy demonstrated cytochalasin D-sensitive colocalization of IQGAP1 with cortical microfilaments. These results, in conjunction with prior evidence that IQGAP1 binds directly to activated Rac and Cdc42, suggest that IQGAP1 serves as a direct molecular link between these GTPases and the actin cytoskeleton, and that the actin-binding activity of IQGAP1 is regulated by calmodulin.

MICROFILAMENTS (MFs)¹ are found in a variety of labile intracellular arrays in nonmuscle cells (10, 38). Near the leading edges of motile cells, MFs are present in ordered bundles, such as filopodia, as well as in loosely organized networks, such as those found in ruffles and lamellipodia. Within the cell interior, MFs may be organized in dense bundles known as stress fibers, which are indirectly connected to cell adhesion sites and have the potential to contract.

Although MFs can be polymerized *in vitro* from actin alone, *in vivo* they invariably encompass actin-binding proteins, each of which influences MF organization in its own specific manner. For example, fimbrin (7) and α -actinin (4) cross-link MFs into bundles, whereas less-ordered MF networks are supported by filamin cross-bridges (18). MF length is regulated by proteins such as gCAP39, which caps MFs (29), and by severin (2) and gelsolin (22), which possess both capping and severing activities. Members of the myosin superfamily serve as molecular motors that transport cargo across the MF surface and allow antiparallel MFs to slide past one another (37).

Interactions between MFs and actin-binding proteins of-

ten appear to be orchestrated responses to extracellular stimuli. The neutrophil reacts to chemotactic agents by enlisting its actin cytoskeleton to move the cell toward the signal (15). Likewise, fibroblasts migrate into wounds by a process that requires transient, repetitive extension of filopodia and lamellipodia toward the wounded region (16).

The signaling pathways that control MF organization appear to be exceedingly complex, and to involve several low molecular weight GTPases as key regulatory factors. Activated, or GTP-bound forms of the Ras-related proteins, Rac and Rho, stimulate formation of lamellipodia (34) and stress fibers (33), respectively. In addition, a closely related GTPase, Cdc42, promotes formation of filopodia when activated by GTP (20, 27). Although each of these three GTPases triggers its own unique set of multiple downstream responses after activation, there is evidence that their actions are coordinated. Apparently, activated Cdc42 stimulates activation of Rac, which in turn stimulates activation of Rho (20, 27). In the context of actin organization, therefore, a primary effect of Cdc42 activation is induction of filopodia, whereas secondary and tertiary effects include Rac-mediated membrane ruffling and Rho-mediated stress fiber formation, respectively.

Some progress has been made toward identifying events that lead to activation of Cdc42, Rac, and Rho. Constitutively active, oncogenic Ras stimulates Rac activation, so yet another low molecular weight GTPase influences MF organization, in this case by acting upstream of Rac and Rho, but independently of Cdc42 (33). Further upstream, GTPase activation is thought to result indirectly from binding of ligands to cell surface receptors. For example,

Please address all correspondence to Dr. George S. Bloom, University of Texas, Southwestern Medical Center, Department of Cell Biology and Neuroscience, 5323 Harry Hines Boulevard, Dallas, TX 75235. Tel.: (214) 648-7680. Fax: (214) 648-8694. e-mail: bloom@utsw.swmed.edu

1. *Abbreviations used in this paper:* FPLC, fast protein liquid chromatography; GAP, GTPase activating protein; MF, microfilament; MT, microtubule.

PDGF, or insulin, acts through PI 3-kinase to stimulate Rac (34); lysophosphatidic acid acts through a tyrosine kinase to stimulate Rho (33); and bradykinin triggers activation of Cdc42 by an unknown mechanism (20).

In comparison to events occurring upstream of GTPase activation, less is understood about events leading from GTPase activation to reorganization of actin. In only one case has a relevant downstream effector of an activated GTPase been directly identified. Very recently, the constitutively active catalytic domain of a Rho-stimulated protein kinase was found to induce stress fibers after microinjection into serum-starved cells (1). The Rho kinase has therefore been implicated as an intermediate between activation of Rho and the resulting assembly of stress fibers. In the cases of Cdc42 and Rac, even less is known. Flowing downstream from activated Cdc42 and Rac are a MAP kinase-dependent pathway and a separate Jun kinase-dependent pathway (3, 12, 26, 28, 42). It is noteworthy that actin reorganization induced by Cdc42 and Rac occurs independently of the Jun kinase pathway (19, 24). Nevertheless, further details of the pathways connecting activated Cdc42 and Rac to cortical actin rearrangement remain shrouded in mystery.

In this report, we describe the discovery, purification, and characterization of a high molecular weight protein that may directly link activated Cdc42 and Rac to actin reorganization. Amino acid sequences of four peptides derived from the protein revealed identity with a previously cloned protein called IQGAP1 (40). Based on the presence of a region with amino acid sequence similarity to catalytic domains of GTPase-activating proteins (GAPs) for Ras, IQGAP1 was initially proposed to be a new Ras-GAP (40). Instead, IQGAP1 was found to bind directly to activated forms of Cdc42 and Rac, but not to active or inactive Ras or Rho, and it inhibits the GTPase activity of Cdc42 (17, 21, 25). Sequence analysis of IQGAP1 indicated the additional presence of four putative calmodulin-binding IQ motifs (40), and direct evidence for calmodulin binding by IQGAP1 has been presented (17).

Here we demonstrate that purified IQGAP1 also binds directly to MFs, and cross-links them into irregular, interconnected bundles that exhibit gel-like properties. We also present evidence that calmodulin inhibits the MF-binding activity of IQGAP1. Finally, the physiological significance of the *in vitro* properties of purified IQGAP1 was bolstered by the finding that IQGAP1 colocalizes with cytochalasin D-sensitive, MF-rich structures in the cell cortex, but is absent from stress fibers. Therefore, the results described here emphasize the likelihood that IQGAP1 is part of a signal transduction network that includes Rac and Cdc42, and is involved in controlling the organization of cortical actin.

Materials and Methods

Materials

Unless specified otherwise, all chemicals and reagents were purchased from Sigma Chemical Co. (St. Louis, MO).

Actin, Tubulin, and Calmodulin

Actin was purified from acetone powders of rabbit skeletal muscle and as-

sembled into F-actin as described (30). The resulting MFs, which typically had a concentration of ~6 mg/ml (~140 μ M) actin, were stored at 4°C. Tubulin was purified from bovine brain by our standard procedure (5), and stored in small aliquots at -80°C. Microtubules (MTs) were polymerized from 12 mg/ml (120 μ M) purified tubulin by the addition of taxol (courtesy of N.R. Lomax, National Cancer Institute, Bethesda, MD) to 180 μ M, and incubation was at 37°C for 30 min. Once they had polymerized, the taxol-stabilized MTs were chilled on ice and used shortly thereafter. Calmodulin was purified from bovine brain as described (13), and was generously supplied by Dr. S. Chacko (University of Pennsylvania, Philadelphia, PA).

MF- and MT-Binding Assays

For identification of MF- and MT-binding proteins in adrenal cytosol (see Fig. 1), MTs and MFs were added to cytosol to a final concentration in both cases of 0.5 mg/ml. After a 30-min incubation on ice, the 1-ml samples were centrifuged for 30 min at 40,000 rpm (86,553 g_{max}) at 4°C in a TL-100 table top ultracentrifuge (Beckman Instruments, Inc., Fullerton, CA) using a TLA 100.3 rotor. The resulting pellets were resuspended in 125 μ l of SDS-PAGE sample buffer, and aliquots were then resolved on a 4-16% polyacrylamide gradient gel (5), which was stained with 0.1% Coomassie brilliant blue R250 (Pierce Chemical Co., Rockford, IL) dissolved in 50% methanol/10% acetic acid/40% water.

To study the binding of purified native IQGAP1 (see below) to F-actin (see Figs. 4-6), 200- μ l samples were centrifuged for 15 min at 30,000 rpm (48,686 g_{max}) at 4°C in an Optima TLX table top ultracentrifuge (Beckman Instruments, Inc.) using a TLA 100.3 rotor. Equal aliquots of the resulting supernatants and pellets were then resolved by SDS-PAGE on 7.5% polyacrylamide gels (23), which were stained with Coomassie brilliant blue R250 as described above.

Peptide Microsequencing

Denatured 190K was purified by preparative SDS-PAGE of MF pellets obtained from adrenal cytosol (see Fig. 1). Gels were briefly stained with an aqueous suspension of Coomassie brilliant blue R250, the 190K band was then excised with a razor blade, and protein was electroeluted from the gel strip. After digestion with endoproteinase lys C (Boehringer Mannheim Biochemicals, Indianapolis, IN), four resulting peptides were purified by HPLC. Partial NH₂-terminal peptide sequences were obtained by automated Edman degradation using a sequencer (model 477A; Perkin Elmer/Applied Biosystems, Norwalk, CT), and programming and chemicals recommended by the manufacturer.

Production of an Antibody to a 190K Peptide

A 10-mer peptide containing nine amino acid residues within peptide 3 (QANAENNEF; see Fig. 2) plus a COOH-terminal cysteine was synthesized. The peptide was then covalently coupled via its cysteine to maleimide-activated keyhole limpet hemocyanin using an Imject Activated Immunogen Conjugation Kit (Pierce Chemical Co.), according to the manufacturer's instructions. Conjugated peptide was emulsified in Titer-Max Adjuvant (Vaxcel, Inc., Norcross, GA), and a rabbit was then immunized five times at 2-4-wk intervals. The final bleed of serum collected from this rabbit was specific for IQGAP1 on immunoblots.

Purification of Native IQGAP1

Fresh bovine adrenal glands, typically ~100 g, were obtained at a local slaughterhouse and stored in ice-cold PEM20 (20 mM Pipes, 2 mM MgCl₂, 1 mM EGTA at pH 6.62) during transit to our laboratory. After removal of the fatty layer, the tissue was minced and homogenized for ~1 min in 1.5 vol of PEM100 buffer (identical to PEM20, but with 100 mM Pipes) supplemented with 1 mM DTT and protease inhibitors (1 μ g/ml each leupeptin, pepstatin A, chymostatin, and 1 mM PMSF). An Omni 5000 tissue grinder (Omni International, Gainesville, VA) was used for homogenization at a speed setting of 2. The homogenate was first centrifuged at 4°C for 20 min at 20,000 rpm (48,384 g_{max}) in a Beckman J2-21 centrifuge using a JA20 rotor. The supernatant was then centrifuged at 4°C for 1.5 h at 44,000 rpm (194,932 g_{max}) in a Beckman L7-55 ultracentrifuge using a 60 Ti rotor. The resulting supernatant (cytosol) was filtered using 0.22- μ m Millex-GV filters (Millipore Corp., Bedford, MA).

IQGAP1 was purified at 4°C from filtered cytosol by three sequential chromatographic steps using fast protein liquid chromatography (FPLC)

and media from Pharmacia LKB Biotechnology Inc. (Piscataway, NJ). IQGAP1 was identified for all chromatographic steps by SDS-PAGE, and by Western blotting (see below) with the peptide antibody described in the previous section. To begin, 50 ml of cytosol were applied at a flow rate of 1 ml/min to a 16-ml SP-Sepharose HP cation exchange column pre-equilibrated with PEM100. The flow through was discarded, and bound protein was eluted in 5-ml fractions using a 400-ml linear gradient of 0–0.6 M NaCl in PEM100. This procedure was then repeated two more times using an additional 50 ml of cytosol at each step. From each of the three identical SP-Sepharose steps, three peak IQGAP1 fractions typically eluted at ~0.25 M NaCl. The peak IQGAP1 fractions from all three SP-Sepharose runs were pooled, concentrated ~10-fold by dialysis against Aquacide II (Calbiochem-Novabiochem Corp., La Jolla, CA), and applied at a flow rate of 0.5 ml/min to a 120-ml Sephacryl-S300 gel filtration column equilibrated with PEM20. Fractions of 2 ml each were collected, and the peak fractions of IQGAP1 were pooled and applied at a flow rate of 1 ml/min to an 8-ml Q-Sepharose anion-exchange column. Protein was eluted from this column as 1-ml fractions using a 5-ml linear gradient of 0–1 M NaCl in PEM100. The IQGAP1 peak typically eluted at ~0.23 M NaCl. Fractions containing purified IQGAP1 were then pooled, dialyzed against PEM20, and concentrated 8–10-fold by dialysis against Aquacide II. Aliquots of the final product were snap frozen in liquid nitrogen, and stored at –80°C.

Immunoblotting

Proteins were resolved by SDS-PAGE and transferred to Immobilon-P membranes (Millipore Corp.) using a Mini-Protean II apparatus (Bio Rad Laboratories, Hercules, CA). To analyze the 190K subunit of IQGAP1, 7% polyacrylamide gels (23) were used. After electrophoresis, gels were equilibrated in transfer buffer (25 mM potassium phosphate, pH 7.0) for 45–60 min, and protein was then transferred at 20 V overnight at 4°C (36). The membrane was then blocked in casein/PBS (PBS at pH 7.4 supplemented with 60 mg/ml casein, 10 mg/ml polyvinylpyrrolidone, 10 mM EDTA, and 2.6 mM NaN₃) for 1 h before being probed with antibodies. PBS and 0.2% Tween 20 was used for antibody dilution and washing steps. Primary antisera included the rabbit anti-190K peptide antiserum described here, as well as a previously described rabbit antiserum made against a bacterially expressed NH₂-terminal fragment of human IQGAP1 (17). Affinity-purified, peroxidase-labeled goat anti-rabbit IgG (Kierkegaard & Perry Laboratories, Inc., Gaithersburg, MD) was used as a secondary antibody, and Luminol chemiluminescence reagents (Pierce Chemical Co.) were used for visualizing immunoreactive protein according to the vendor's instructions.

Immunoblotting of calmodulin was performed exactly as described (35) after resolving proteins on 14% polyacrylamide gels (23). Monoclonal anti-calmodulin (Upstate Biotechnology Inc., Lake Placid, NY) and affinity-purified peroxidase-labeled goat anti-mouse IgG (Pierce Chemical Co.) were used as primary and secondary antibodies, respectively. Calmodulin was detected on blots by a chemiluminescent assay, as described for 190K.

Quantitation of Gels and Immunoblots

Silver- and Coomassie-stained gels, and chemiluminescent immunoblots were digitally photographed using a Dage-MTI CCD-72 camera (Michigan City, IN) as an input device for a Power Macintosh 7600 computer (Apple, Cupertino, CA). In all cases in which quantitation was performed, a concentration series of known amounts of protein (IQGAP1, actin, or calmodulin) was included on the gel or blot. NIH Image software (National Institutes of Health, Bethesda, MD) was used for image capturing, and for quantitation of bands on blots or gels.

Sedimentation Equilibrium

A 100- μ l aliquot of purified IQGAP1 supplemented with 5 mg/ml dextran (70,000 mol wt) was layered on top of fluorocarbon and was overlaid with mineral oil in a 0.5-ml centrifuge tube for a Beckman TLS-55 swinging bucket rotor. The sample was spun for 3 h at 12,000 rpm (12,338 g_{max}) followed by 63 h at 6,000 rpm (3,084 g_{max}) in a Beckman Optima TLX 120 table top ultracentrifuge at 4°C. Samples of 7 μ l each were then collected using a Brandel FR-115 Centrifuge Tube Microfractionator (Biomedical Research and Development Laboratories, Inc., Gaithersburg, MD). Aliquots of protein-containing fractions were then resolved by SDS-PAGE (23) on 7% polyacrylamide gels. The gels were initially stained with silver (6), were then destained completely using Rapid-Fix (Eastman Kodak

Co., Rochester, NY), and finally were restained using Coomassie brilliant blue R250. Protein quantities in each lane were measured as described above. Data were plotted separately for five silver- and six Coomassie-stained fractions (see Fig. 7). Linear regression analysis was used to calculate best fit straight lines for each set of data, and molecular weights were calculated from the slopes of the lines using the following equation (9).

$$\frac{d \ln C}{dr^2} = \frac{m(1 - \bar{v}\rho)\theta^2}{2RT}$$

where $d \ln C/dr^2$ = the slope, m = molecular weight, \bar{v} = partial specific volume ($0.73 \text{ cm}^3 \cdot \text{g}^{-1}$), ρ = solution density ($1.0 \text{ g} \cdot \text{cm}^{-3}$), θ = angular velocity (in radians), R = the gas constant ($8.31 \times 10^7 \text{ erg} \cdot \text{deg}^{-1} \cdot \text{mol}^{-1}$), and T = temperature (277°K).

Falling Ball Viscometry

To determine whether IQGAP1 cross-links F-actin, the viscosity of solutions containing IQGAP1, F-actin, or combinations of both were assayed by falling ball viscometry (31). The F-actin concentration was held constant at 10 μ M polymerized actin, the IQGAP1 concentration was varied from 31.25 to 500 nM, and the capillary tube was held at an angle of 30°.

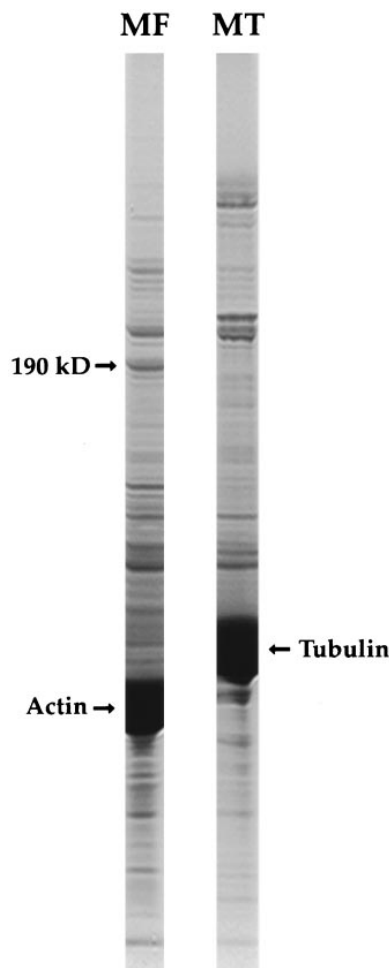


Figure 1. A 190-kD putative actin-binding protein is present in bovine adrenal tissue. MFs assembled from purified rabbit muscle actin, or MTs assembled with taxol from purified bovine brain tubulin, were added to bovine adrenal cytosol at 4°C. After centrifugation, the MT and MF pellets were resuspended and analyzed by SDS-PAGE. As can be seen, a prominent 190-kD polypeptide was present exclusively in the MF pellet.

Electron Microscopy

F-actin at 0.07 mg/ml (1.6 μ M) was incubated for 30 min at room temperature in the absence or presence of purified IQGAP1 at 0.15 mg/ml (0.4 μ M native protein). Samples were fixed by addition of glutaraldehyde and ρ -formaldehyde to 2 and 1%, respectively, and 4- μ l aliquots were placed on Formvar and carbon-coated grids that had been glow-discharged using a Balzers Med 010 Mini Deposition System (Balzers Union Ltd., Balzers, Liechtenstein). Grids were rinsed successively with three drops each of distilled water, 0.2 mg/ml cytochrome C, and 2% uranyl acetate. Excess stain was removed by blotting from the side with No. 1 filter paper (Whatman, Maidstone, England). Grids were examined on a JEOL 1200 EX electron microscope (JEOL Ltd., Tokyo, Japan).

Immunofluorescence Microscopy

CV-1 (African green monkey kidney), NRK (normal rat kidney), NIH 3T3 (mouse fibroblast), and MDCK (canine kidney) cells were maintained in DME (GIBCO BRL, Grand Island, NY) supplemented with 10% calf serum (Hyclone, Logan, UT) and gentamycin. For immunofluorescence, cells were grown on No. 1 thickness glass coverslips, and were fixed and stained as described previously (11). A rabbit antiserum raised against a bacterially expressed NH₂-terminal fragment of IQGAP1 (17) was used as primary antibody, and affinity-purified rhodamine-labeled goat anti-rabbit IgG (Organon Teknica, Durham, NC) was used as the secondary antibody. To visualize MFs, Bodipy-phalloidin (Molecular Probes Inc., Eugene, OR) was added to the secondary antibody solution. In some cases, cells were treated with 5 μ g/ml cytochalasin D for 30 min before fixation.

Digital micrographs were acquired using a C5985 cooled CCD, a C6391 camera controller, and an Argus 20 image processor (all from Hamamatsu Photonics, Bridgewater, NJ) that were connected via the Argus 20 to the SCSI port of a Power Macintosh 8500 computer (Apple). Images were imported into the computer using Adobe Photoshop software (Adobe Systems, Mountain View, CA) and a Photoshop plug-in from Hamamatsu Photonics.

Results

Identification of an MF-associated Protein in Adrenal Cytosol as IQGAP1

To identify adrenal proteins that may associate with the cytoskeleton *in vivo*, bovine adrenal cytosol was supplemented with either MFs, assembled from purified rabbit muscle actin, or MTs, assembled from purified bovine brain

tubulin with the aid of taxol. After a centrifugation step, the MF and MT pellets were analyzed by SDS-PAGE. As illustrated in Fig. 1, a prominent band of \sim 190,000 mol wt (190K) was found exclusively in the MF pellets. Because we were not aware of any major actin-binding proteins of that size, protein present in this band was electrophoretically eluted and then digested with endoproteinase lys C. Four peptides that were purified by reverse-phase HPLC yielded sequences of 27-, 20-, 13-, and 20-amino acid residues.

As illustrated in Fig. 2, comparison of the peptide sequences with the GenBank/EMBL/DDBJ data bank indicated high identity of bovine 190K with human IQGAP1, a 1,658-amino acid residue protein that contains four potential calmodulin-binding IQ domains and a region homologous to catalytic domains of GTPase-activating proteins, or GAPs (40). The sequences of peptides 1, 2, and 3 match sequences within the NH₂-terminal third of IQGAP1, while peptide 4 corresponds to a region within the COOH-terminal third of IQGAP1. Of the 80 amino acid residues present in the four 190K peptides, 71 are identical to equivalent residues in human IQGAP1. Sequences corresponding to peptides 1 and 4 are also found in human IQGAP2, a protein which is 62% identical to IQGAP1 (8). IQGAP2 was not likely to be a major component of the electroeluted adrenal protein, however, because sequences related to adrenal peptides 2 and 3 are not present in IQGAP2, which was reported to be abundant only in liver (8).

Purification of Native IQGAP1

All previous studies of IQGAP1 have made use of either unpurified native or recombinant protein (17, 21, 25, 40). To facilitate characterization of the native protein, we developed a method to purify IQGAP1 from adrenal cytosol by FPLC. The method entailed sequential cation exchange (SP Sepharose), gel filtration (Sephacryl S-300), and anion exchange (Q Sepharose) columns. To aid identification of IQGAP1 during each chromatography step, we generated an anti-IQGAP1 antibody by immunizing a rabbit with a

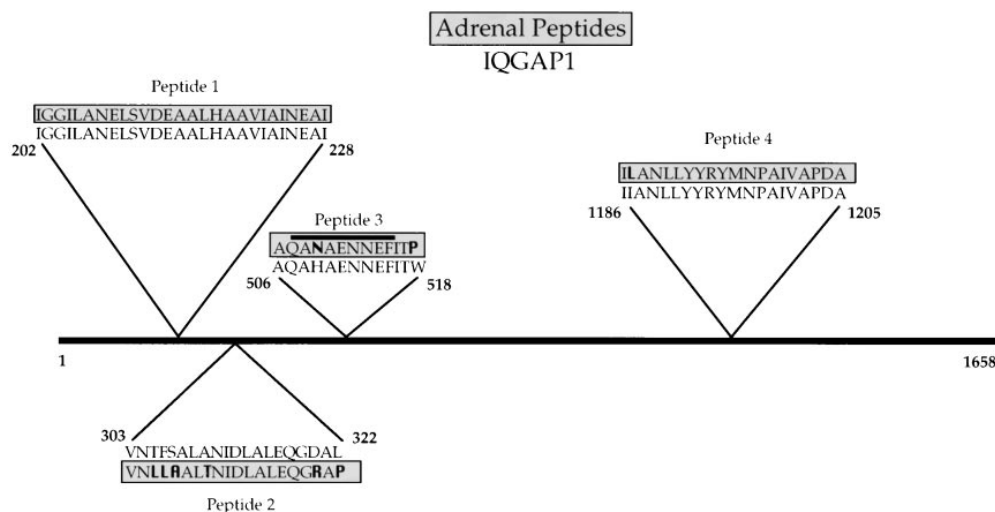


Figure 2. The 190-kD polypeptide is equivalent to IQGAP1. The 190-kD polypeptide was purified in denatured form by preparative SDS-PAGE, electroeluted from the gel, and digested in solution with endoproteinase lys C. Four peptides were purified by HPLC and sequenced. Comparison of the peptide sequences with the GenBank/EMBL/DDBJ data bank indicated high identity of the bovine adrenal protein with human IQGAP1, a 1,658-amino acid residue protein that contains four potential calmodulin-binding IQ domains, and a region

homologous to catalytic domains of GAPs (40). Sequences corresponding to peptides 1 and 4 are also found in human IQGAP2, a protein which is 62% identical to IQGAP1, but is reportedly abundant only in liver (8). A 9-mer peptide corresponding to the highlighted residues within peptide 3 was used as an immunogen for the production of an anti-IQGAP1 antibody.

9-mer peptide that corresponded to amino acid residues 2–10 of peptide 3 (see Fig. 2). This peptide is not found in IQGAP2, and the resulting antiserum is therefore specific for IQGAP1.

As illustrated in Fig. 3 A, an ~190-kD band that reacts with the antibody became progressively enriched through successive stages of the purification procedure. Similar results were obtained using a previously described anti-IQGAP1 (17) which was also used in the present study for immunofluorescence (see Fig. 10). Beginning with 100 g of bovine adrenal glands containing both cortical and medullary tissue, the final yield of protein has typically been 0.6–0.8 mg.

When analyzed by SDS-PAGE, the final product usually contained a few variable minor bands in addition to the major 190K band, which occasionally was resolved as two closely spaced electrophoretic species. The presence of four IQ motifs in 190K (40) raised the possibility that native purified IQGAP1 contains 4 mol of tightly bound calmodulin per mol of 190K subunit. As shown in Fig. 3 A, purified IQGAP1 contained copurifying calmodulin, but at a low stoichiometric ratio to 190K. Calmodulin levels were measured in four independent preparations of purified IQGAP1. In three examples, the molar ratios of calmodulin to 190K were 1:15, 1:24, and 1:39, respectively, while calmodulin was undetectable in the fourth preparation.

The calmodulin present in pooled Q-Sepharose fractions of IQGAP1 could have represented the leading or trailing edge of a contaminating pool of calmodulin that was not directly associated with 190K. Alternatively, the calmodulin could have been a copurifying, albeit substoichiometric subunit of IQGAP1. To distinguish between these two possibilities, Q-Sepharose fractions that contained 190K were analyzed by Western blotting with antic-calmodulin. As demonstrated in Fig. 3 B, levels of both calmodulin and 190K peaked in fraction 29 of the Q-Sepharose column, although compared to the 190K peak, the calmodulin peak was skewed toward later-eluting column fractions. Calmodulin thus appears to be a bonafide substoichiometric subunit of purified IQGAP1, and we suspect that the Q-Sepharose column fractionated IQGAP1 into an early-eluting, calmodulin-deficient pool, and a late-eluting, calmodulin-enriched pool (see Discussion).

Purified IQGAP1 Binds to F-actin With High Affinity

To account for the presence of IQGAP1 in MF pellets isolated from adrenal cytosol (as in Fig. 1), IQGAP1 could have bound directly to MFs, or indirectly via one or a series of linking proteins. To distinguish between these possibilities, solutions of purified IQGAP1 were centrifuged in the absence or presence of F-actin, and the supernatants and pellets were then analyzed by SDS-PAGE. Fig. 4 illustrates the results of a typical experiment. At a concentration of 0.15 mg/ml, nearly all of the IQGAP1 remained soluble when MFs were absent, but approximately two thirds of the IQGAP1 was pelleted in the presence of 0.14 mg/ml (3.2 μ M) F-actin. In other experiments, as much as ~85% of the IQGAP1 was able to bind F-actin.

To begin the task of characterizing the kinetic and thermodynamic properties of interactions between IQGAP1 and F-actin, 0.15 mg/ml IQGAP1 was mixed with variable amounts of F-actin, and the samples were centrifuged. The

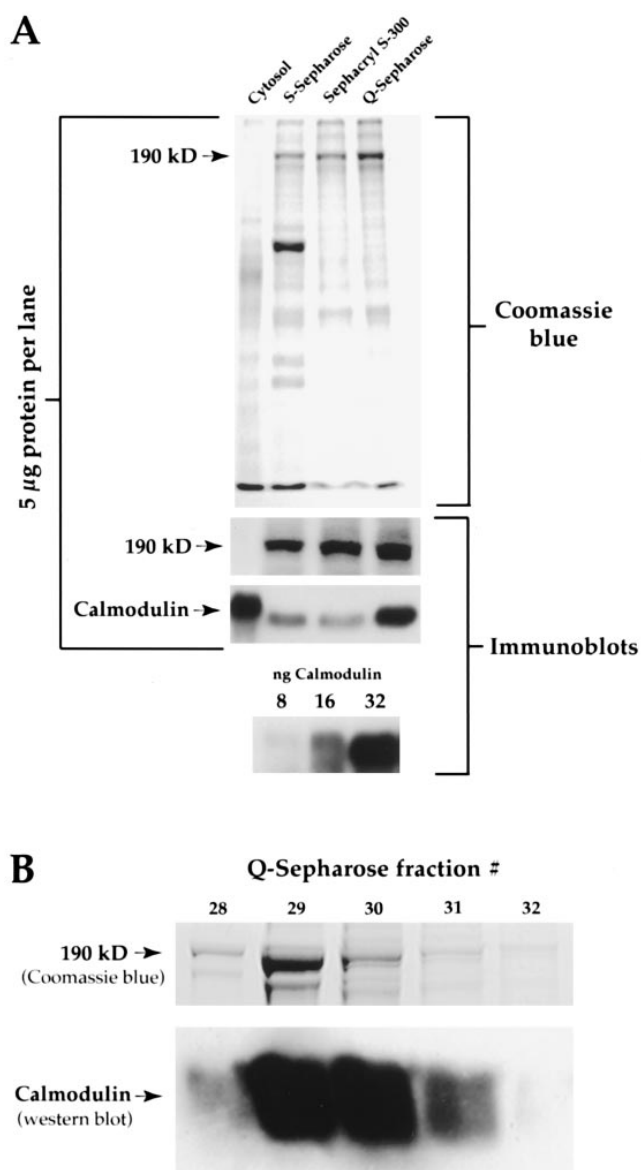


Figure 3. Purified, native IQGAP1 contains copurifying, but substoichiometric calmodulin. (A) Native IQGAP1 was purified from bovine adrenal cytosol by FPLC using sequential cation exchange (S-Sepharose), gel filtration (Sephacryl S-300), and anion exchange (Q-Sepharose) columns. A Coomassie blue-stained gel of 5- μ g samples of cytosol and each of the three column steps are shown in the upper part of the figure. The lower part of the figure illustrates corresponding Western blots for the 190-kD IQGAP1 subunit and calmodulin, as well as a calmodulin concentration series (8, 16, and 32 ng). Note that the 190-kD subunit was undetectable in cytosol at the exposure shown here, and that it became progressively enriched throughout the purification procedure. Note also that 5 μ g of purified IQGAP1 contained ~20 ng of calmodulin, or an ~1:20 molar ratio of calmodulin to the 190-kD polypeptide. (B) To determine whether the calmodulin present in purified IQGAP1 represented a copurifying subunit of the native molecule or a trace contaminant, Q-Sepharose fractions that contained the 190-kD polypeptide were analyzed by Western blotting with antic-calmodulin. Coelution of the 190-kD polypeptide and calmodulin were observed, although the calmodulin peak was more skewed than the 190-kD peak toward late-eluting fractions (see Discussion). Calmodulin thus appears to be a bona fide, albeit substoichiometric subunit of purified native IQGAP1.

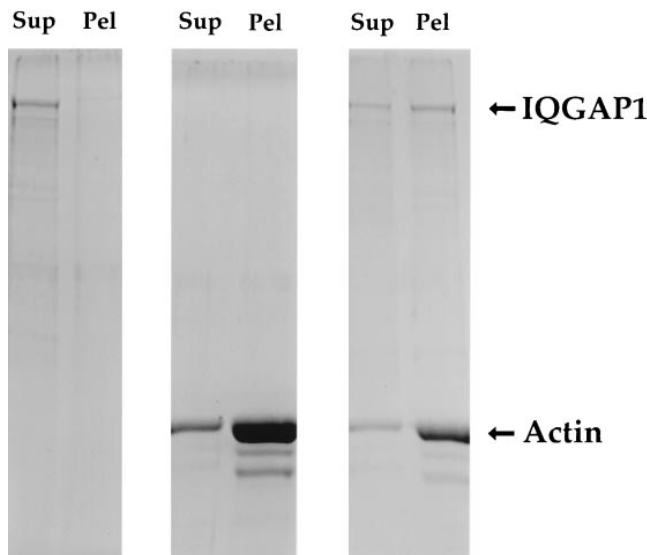


Figure 4. Purified IQGAP1 binds directly to F-actin. To account for the presence of IQGAP1 in MF pellets isolated from adrenal cytosol (see Fig. 1), IQGAP1 could have associated directly or indirectly with F-actin. To distinguish between these possibilities, purified IQGAP1 at 0.15 mg/ml was centrifuged alone (*left*) or in combination with 0.14 mg/ml (3.2 μ M) F-actin (*right*), and the supernatants (*Sup*) and pellets (*Pel*) were analyzed by SDS-PAGE. As a control, F-actin alone at 0.28 mg/ml (6.4 μ M) was also centrifuged in parallel (*center*). As shown here, purified IQGAP1 bound directly to F-actin.

pellets were then resuspended to the original sample volumes, and the amounts of IQGAP1 and F-actin in each pellet were determined by quantitative SDS-PAGE, as described in detail in Materials and Methods. A plot of the percentage of IQGAP1 bound vs F-actin is shown in Fig. 5. Note that 50% of the IQGAP1 that was able to bind F-actin was bound at an F-actin concentration of \sim 40 nM. When the data were reanalyzed by the Scatchard method (9), a curved or multiphasic plot was obtained (not shown), implying the existence of multiple classes of binding sites on IQGAP1 for F-actin. The fact that half of the IQGAP1 bound to 40 nM F-actin should thus be regarded as an indication of high affinity binding, but 40 nM is probably not a reliable estimate of the dissociation constant.

Calmodulin Partially Inhibits Binding of IQGAP1 to F-actin

To determine whether calmodulin influences the association of IQGAP1 with F-actin, we performed a binding assay in which 0.19 mg/ml IQGAP1 (1 μ M 190K subunit; 4 μ M IQ domains) plus 10 μ M F-actin were centrifuged in the absence of additional factors, or in the presence of \sim 250 μ M free calcium, 40 μ M calmodulin (160 μ M calcium binding sites), or calcium plus calmodulin. As illustrated in Fig. 6, 64% of the IQGAP1 pelleted in the absence of other factors, while binding in the presence of calcium rose slightly to 75%. Binding was potently inhibited by calmodulin, and demonstrably, but less so, by calcium plus calmodulin. Only 36% of the total IQGAP1 bound to F-actin in the presence of calmodulin alone, while 45% bound in the presence of calmodulin plus calcium.

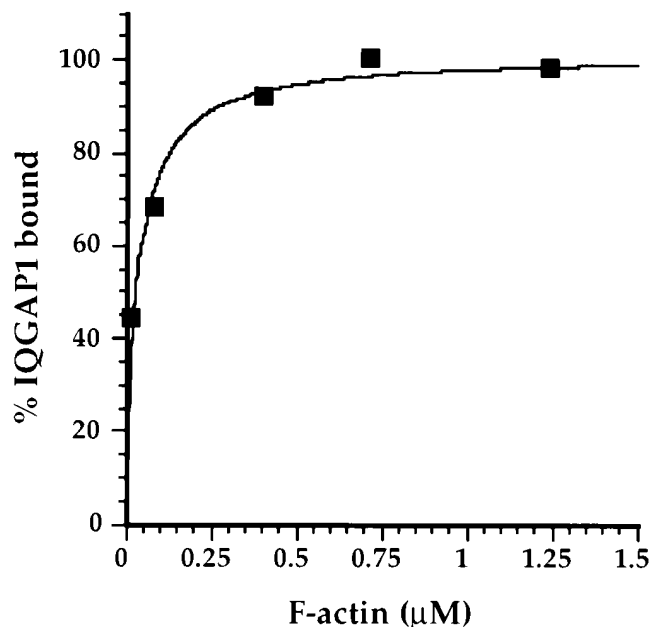


Figure 5. IQGAP1 binds F-actin with high affinity. 0.15 mg/ml IQGAP1 was mixed with various amounts of F-actin, and the samples were centrifuged. The pellets were then resuspended to the initial sample volumes, and the amounts of IQGAP1 and F-actin in each pellet were determined by quantitative SDS-PAGE. A plot of the percentage of IQGAP1 bound vs F-actin is shown here, and the data were fitted to a hyperbolic curve. In this experiment, two-thirds of the total IQGAP1 was able to bind F-actin, and 0.1 μ g/ml IQGAP1 was therefore defined as 100% bound. Note that 50% of the binding-competent IQGAP1 was bound at \sim 40 nM F-actin. When the data were reanalyzed by the Scatchard method, a curved or multiphasic plot was obtained (not shown), implying the existence of multiple classes of binding sites on IQGAP1 for F-actin. The fact that half of the IQGAP1 bound to 40 nM F-actin should thus be regarded as an indication of high affinity binding, but 40 nM is probably not a reliable estimate of the dissociation constant.

The Native IQGAP1 Molecule Comprises Two 190K Subunits

To estimate the molecular weight of native IQGAP1, purified protein was analyzed by sedimentation equilibrium in a table top ultracentrifuge (32). Quantitative SDS-PAGE was used to determine the relative levels of IQGAP1 in fractions collected immediately after centrifugation. Reliable quantitative data were obtained for the five least dense fractions by silver staining, and for the six densest fractions by Coomassie blue staining. As shown in Fig. 7, the silver and Coomassie data yielded estimated molecular weights of 358,653 and 401,864, respectively, or an average of 380,256. These values are most readily explained by a molecule that comprises two subunits of \sim 190 kD each.

IQGAP1 Cross-links F-actin into Gel-like Networks of Interconnected Bundles

The finding that each native IQGAP1 molecule comprises two \sim 190-kD subunits—both of which presumably bind F-actin—led us to suspect that IQGAP1 is capable of cross-linking MFs, and might explain the complex Scatchard results if the two binding sites had coupled affinities.

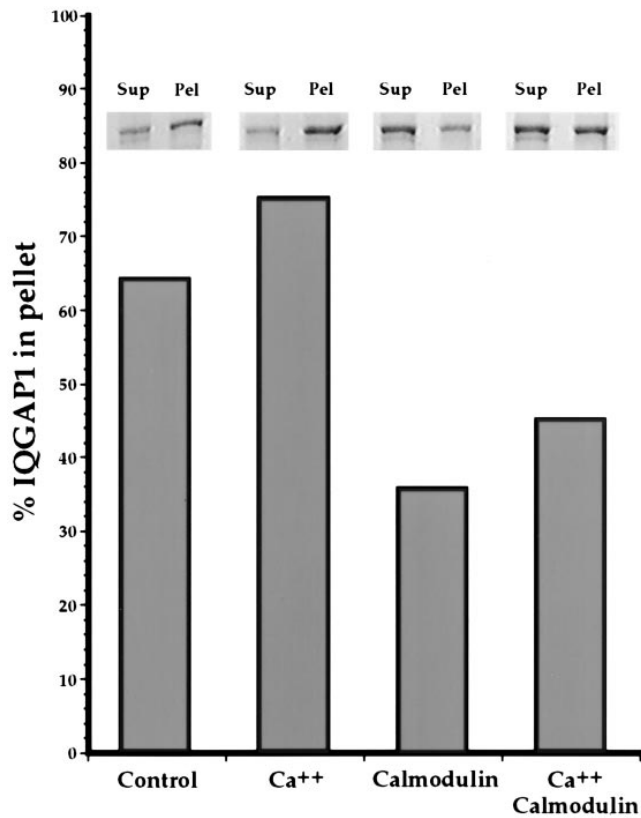


Figure 6. Calmodulin inhibits binding of IQGAP1 to F-actin. 0.19 mg/ml IQGAP1 (1 μ M 190K subunit; 4 μ M IQ domains) plus 10 μ M F-actin were centrifuged in the absence of additional factors, or in the presence of calcium (\sim 250 μ M above the EGTA concentration), 40 μ M calmodulin (160 μ M calcium binding sites), or calcium plus calmodulin. Note that 64% of the IQGAP1 pelleted in the absence of other factors, while binding in the presence of calcium rose slightly to 75%. Binding was potently inhibited by calmodulin, and demonstrably, but less so, by calcium plus calmodulin. Only 36% of the total IQGAP1 bound to F-actin in the presence of calmodulin alone, while 45% bound in the presence of calmodulin plus calcium.

To test for cross-linking activity, two independent assays were used to analyze the structural properties of mixtures of purified IQGAP1 and F-actin. The first method, falling ball viscometry, reveals proteins that cross-link MFs into gel-like networks (31). As shown in Fig. 8, the viscosity of 10 μ M polymerized actin was low, and was increased slightly in a dose-dependent manner by addition of IQGAP1 up to a concentration of 250 nM. At 500 nM IQGAP1, the next highest concentration that was tested, the viscosity became infinite, indicating that a gel had formed. About 65% of the IQGAP1 used for these experiments was competent to bind actin, so gelation occurred at a molar ratio of polymerized actin to IQGAP1 of \sim 33–67. F-actin was able to bind much higher levels of IQGAP1, as indicated by quantitative electrophoretic analysis of centrifuged complexes of F-actin and IQGAP1 (as in Fig. 4). Molar ratios of IQGAP1 to actin as high as 1:3 were observed in such pellets (data not shown).

Negative stain EM provided additional independent evidence that IQGAP1 does, indeed, cross-link F-actin into networks. As illustrated in Fig. 9, striking bundles of MFs

were observed when 0.4 μ M IQGAP1 was mixed with 1.6 μ M polymerized actin. The bundles were of variable diameter and length, and often appeared to form intricate, interconnected branches. Bundles were not observed when either F-actin (Fig. 9) or IQGAP1 (not shown) was analyzed individually by negative stain EM.

IQGAP1 Is Localized on Cytochalasin D-sensitive MFs Confined to the Cell Cortex

The *in vitro* properties of IQGAP1 summarized in Figs. 1, 3, 4–6, 8, and 9 implied that the protein interacts directly with MFs *in vivo*. To evaluate that possibility, cultured mammalian cells were stained for immunofluorescence microscopy. A previously described antibody to IQGAP1 (17) was used for these experiments, because our new anti-peptide antibody that works well for immunoblotting (Fig. 3) does not work for immunofluorescence. Cells were also counterstained with Bodipy-phalloidin, which binds to MFs, but not to disassembled actin. Fig. 10 demonstrates typical results which were obtained using African green monkey kidney (CV-1) cells cultured in standard, serum-containing medium. Lamellipodia located at the outer margins of nearly all cells and at sites of cell-cell contact were brightly stained by anti-IQGAP1. Faint, diffuse staining of the cytoplasm by anti-IQGAP1 was also observed. In a limited number of cells, putative ruffles located at the upper cell surface were also strongly immunoreactive with anti-IQGAP1. Bodipy-phalloidin stained the IQGAP1-positive structures brightly, confirming their identification as MF-rich lamellipodia and ruffles. Bodipy-phalloidin also yielded brilliant staining of stress fibers, but in stark contrast, stress fibers were not stained by anti-IQGAP1. Similar results were obtained using NRK (normal rat kidney), NIH 3T3 (mouse fibroblast), and MDCK (canine kidney) cells (data not shown), and were reported recently by other laboratories (17, 21). To determine whether the distribution of IQGAP1 was sensitive to drugs that disrupt MFs, CV-1 cells were exposed to 5 μ g/ml cytochalasin D for 30 min (Fig. 10). Most MFs were depolymerized, as judged by staining with Bodipy-phalloidin. Consistent with the hypothesis that IQGAP1 is localized on cortical MFs, IQGAP1-positive structures were dramatically reduced in abundance in cytochalasin D-treated cells.

Discussion

The low molecular weight GTPases, Rac and Cdc42, induce dramatic changes in the organization of cortical MFs when they are activated by GTP. Rac stimulates formation of ruffled membranes, especially lamellipodia (34). These thin veils of MF-rich cytoplasm are found at the forward edges of motile cells and lead the cell in its advance along the underlying substratum. By comparison, Cdc42 promotes the formation of filopodia (20, 27), the shafts of which contain tightly bundled MFs. While the effects of activated Rac and Cdc42 on the actin cytoskeleton are well documented, little progress has been made toward defining the biochemical events that begin at GTPase activation and are ultimately manifest as reorganization of cortical MFs. In particular, molecules that link Rac and Cdc42 to the actin cytoskeleton had not been identified until now.

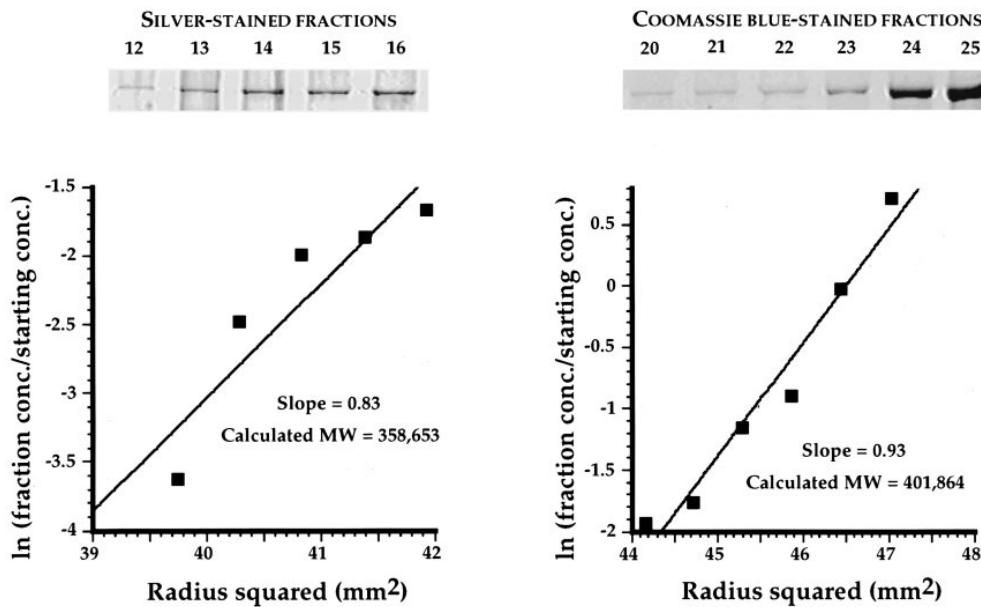


Figure 7. Two 190-kD polypeptides are present in each native IQGAP1 molecule. Sedimentation equilibrium in a table top ultracentrifuge was used to determine the molecular weight of native purified IQGAP1 (see Materials and Methods for details). Quantitative densitometry of a silver-stained gel of the five least dense fractions (*left*) and of a Coomassie blue-stained gel of the six densest fractions (*right*) yielded data that were plotted as indicated on the two graphs. The slope of each graph is a function of molecular weight, which was calculated to be 358,653 and 401,864 for the silver and Coomassie stains, respectively. The average of these two figures is 380,256, and the data are most readily explained by a native IQGAP1 molecule that comprises two \sim 190-kD subunits.

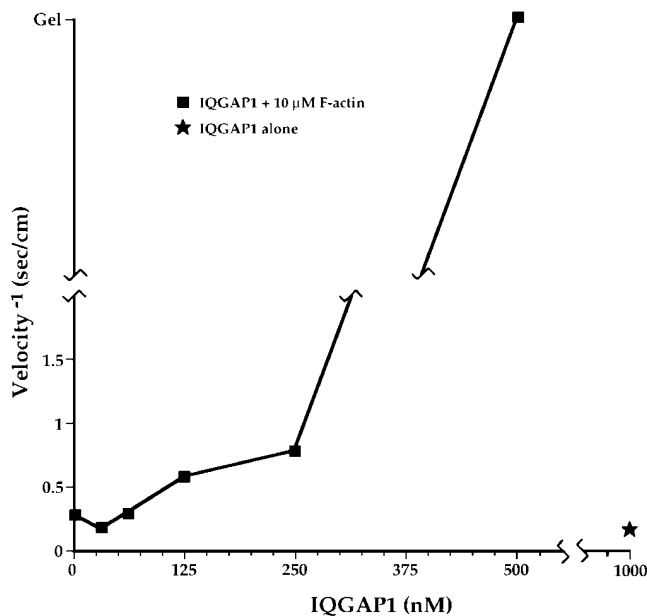


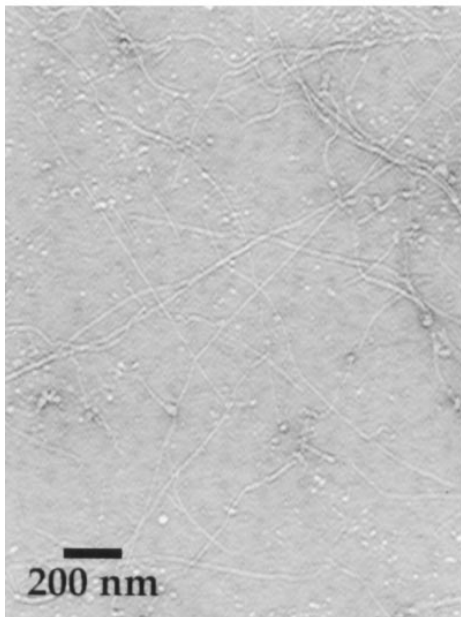
Figure 8. Purified IQGAP1 causes F-actin to gel. F-actin at 10 μ M was mixed with various concentrations of purified IQGAP1 ranging from 0–500 nM, and each sample was analyzed by falling ball viscometry (see Materials and Methods for details). Note that the ball was able to travel through a mixture of 10 μ M actin plus 250 nM IQGAP1, but that a gel-like state, in which the ball did not move, was achieved at 500 nM IQGAP1. Note also that the ball moved readily through a sample of 1 μ M IQGAP1 in the absence of F-actin.

In the present report, we demonstrate that IQGAP1 (40), a molecule that previously was shown to bind directly to activated Cdc42 and Rac (17, 21, 25), also interacts with MFs. Purified IQGAP1 binds directly and with high affinity to F-actin (Figs. 4–6), and cross-links the actin filaments into loosely organized bundles and meshworks that behave physically like gels (Figs. 8 and 9). In cultured mammalian cells, IQGAP1 is localized on specific structures within the actin cytoskeleton. By immunofluorescence (Fig. 10), IQGAP1 appears to be especially abundant inside of membrane ruffles, regardless of whether they are motile lamellipodia, are located at sites of cell–cell contact, or represent patches of active membrane on the upper surface of the cell. In contrast, IQGAP1 appears to be virtually absent from the most conspicuous MF-rich structures in the cell—stress fibers. The fact that the IQGAP1-positive structures are sensitive to cytochalasin D emphasizes the likelihood that in vitro interactions of IQGAP1 with F-actin are representative of direct interactions of IQGAP1 with cortical MFs in vivo.

The location of the actin binding sites within the IQGAP1 molecule has not yet been established. A leading candidate, however, is a region near the NH₂ terminus of the 190K subunit that has homology to MF-binding domains of calponin, spectrin, and a few other rod-shaped, multimeric actin-binding proteins (17). The 190K polypeptide might contain multiple MF-binding sites, but because each IQGAP1 molecule contains two 190K subunits (Fig. 7), the native molecule must have a minimum of two binding sites for MFs. That fact alone could account for the MF cross-linking activity of IQGAP1.

The localization data shown in Fig. 10 are consistent with the specificities of IQGAP1 for binding to low molecular

F-actin



F-actin + IQGAP1

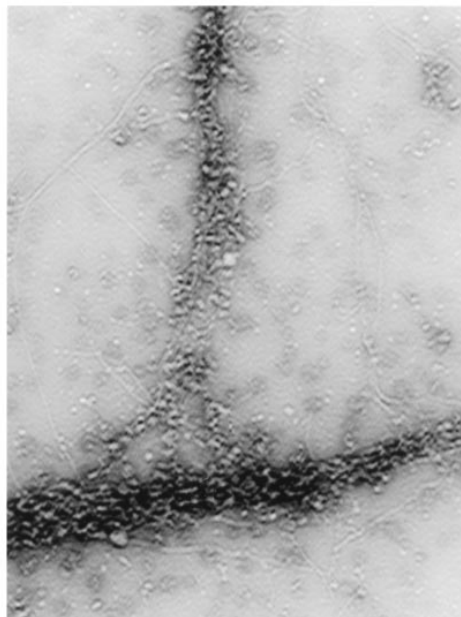


Figure 9. Purified IQGAP1 cross-links F-actin into bundles. Negative stain EM was used to analyze F-actin alone (1.6 μ M polymerized actin) or in combination with purified IQGAP1 (0.4 μ M). Striking bundles of F-actin were observed when IQGAP1 was present. The bundles were of variable diameter and length, and often appeared to form intricate interconnected branches. IQGAP1 alone did not form bundles (not shown). Bar, 200 nm.

weight GTPases *in vitro*. In particular, the apparent enrichment of IQGAP1 in lamellipodia and ruffles is predicted by its ability to bind activated Rac (17, 21, 25). Although activated Cdc42, which stimulates formation of filopodia, has been reported to bind more avidly than activated Rac to IQGAP1 (17), we rarely observed filopodia in cultured cells grown continuously in serum-containing media. We were able to induce filopodia in a limited number of serum-starved cells by briefly exposing the cells to bradykinin (20) or serum, however, and those filopodia were strongly immunoreactive with anti-IQGAP1 (Sontag, J.-M., and G.S. Bloom, unpublished observations). Although our results regarding the association of IQGAP1 with filopodia must be regarded as preliminary, they support the hypothesis that IQGAP1 interacts with Cdc42 not only in the test tube (17, 21, 25), but in cells as well. Likewise, the lack of stress fiber staining by anti-IQGAP1 mimics its inability *in vitro* to bind Rho (17, 25), a GTPase which stimulates assembly of stress fibers when it is activated (33).

The 190K subunit of IQGAP1 contains four putative IQ motifs (40), which typically function as binding sites for calmodulin. Recombinant IQGAP1 was able to bind calmodulin (17), so the low levels of calmodulin that were present in our most highly purified preparations of native IQGAP1 represent a puzzle. Whereas a 4:1 molar ratio of calmodulin to 190K was predicted, the average ratio for three preparations of IQGAP1 that contained calmodulin was 1:26. Despite this paucity of calmodulin, comparison of the elution profiles of calmodulin and 190K from Q-Sepharose columns at the final fractionation step indicated that the calmodulin present in purified IQGAP1 probably is bound to 190K. Although both calmodulin and 190K peaked in the same Q-Sepharose fraction, the calmodulin peak was skewed toward late-eluting fractions compared to the peak of 190K (Fig. 3 *B*). This observation may indicate that relative to early fractions of IQGAP1, late fractions

were enriched for highly acidic calmodulin subunits, were thereby more negatively charged, and consequently bound more tightly to the positively charged Q-Sepharose column.

We do not yet understand why so little calmodulin is present in purified IQGAP1. One possible explanation that must be seriously considered, however, is that much more calmodulin is bound to IQGAP1 *in vivo*, but that the binding is relatively weak and calmodulin may progressively dissociate from 190K throughout the purification procedure. It is also worth considering the possibility that only a fraction of the IQ motifs are specific for calmodulin, and that the remainder interact with other reversibly associating factors.

The functional significance of IQGAP1-associated calmodulin remains to be established. Nevertheless, the observation that exogenous calmodulin inhibited binding of purified IQGAP1 to F-actin (Fig. 6) suggests that calmodulin is a negative regulator *in vivo* of interactions between IQGAP1 and MFs. The finding that calmodulin inhibited binding of IQGAP1 to F-actin more potently in the absence of calcium than in its presence (Fig. 6) implies that calcium inhibits binding of calmodulin to IQGAP1. In that respect, the IQ motifs in IQGAP1 resemble those found in myosins, which usually bind calmodulin most avidly in the absence of calcium (41).

The data presented here, along with prior evidence regarding the properties of IQGAP1 (17, 21, 25), prompt speculation about how 190K dimers and reversibly associating cofactors, such as calmodulin, Cdc42, and Rac, might interact to regulate cortical MFs. In quiescent cells, most IQGAP1 might be associated with calmodulin and thus would not be bound to MFs. Consequently, the cells would contain few, if any, filopodia or ruffled membranes. Stimulation of the cells by appropriate extracellular signals would activate GTPases, such as Cdc42 and Rac, which then would bind to IQGAP1. GTPase association might stimulate MF binding by IQGAP1, either by inducing dissociation of

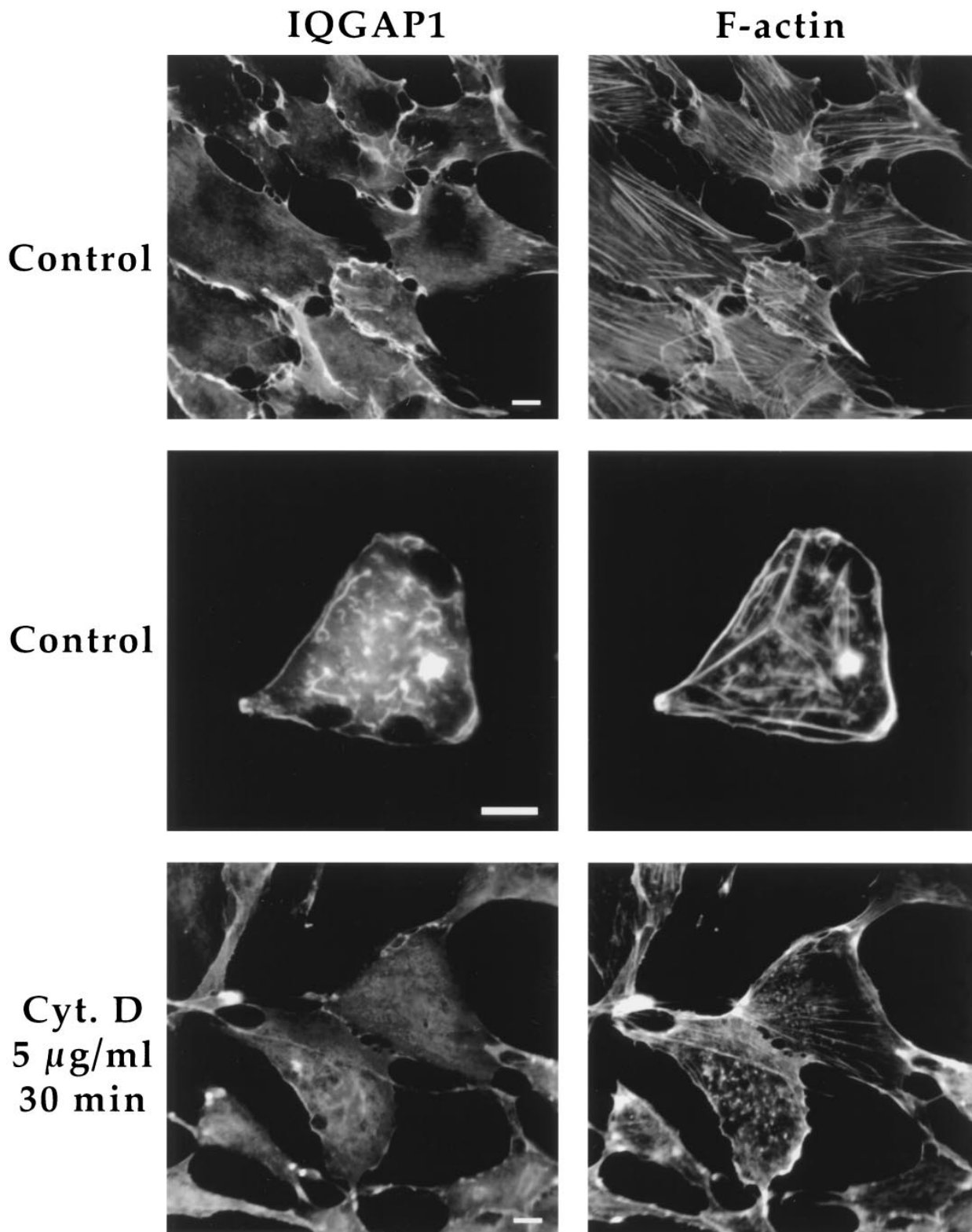


Figure 10. IQGAP1 colocalizes with cytochalasin D-sensitive microfilaments in lamellipodia and ruffles, but not in stress fibers. CV-1 cells were stained with a rabbit antibody to IQGAP1 (17) followed by rhodamine-labeled goat anti-rabbit IgG and Bodipy-phalloidin (to visualize F-actin). Intense IQGAP1 and F-actin staining was colocalized in lamellipodia located at cell margins (*top row*), and in ruffles located on the upper surfaces of some cells (*middle row*). Weak, diffuse staining by anti-IQGAP1 was also seen throughout the cytoplasm, and may represent soluble protein. Stress fibers, which contain densely packed MFs and were brightly stained by Bodipy-phalloidin, were not stained by anti-IQGAP1. After a 30-min exposure to 5 μ g/ml cytochalasin D, which caused F-actin to depolymerize, cells were substantially depleted of IQGAP1-positive structures, and of stress fibers as well (*bottom row*). Bar, 10 μ m.

calmodulin or by negating the inhibitory effects of bound calmodulin on the actin-binding activity of IQGAP1. Transient calcium rises induced by cellular stimulation might also contribute to dissociation of calmodulin from IQGAP1. Finally, GTP hydrolysis might trigger release of Cdc42 or Rac from IQGAP1, and return IQGAP1 to a ground state characterized by a high level of bound calmodulin and minimal MF-binding activity. Although presently this scheme is highly speculative, it establishes a set of testable hypotheses that are now being investigated by a combination of in vitro biochemical and cell biological approaches.

Regardless of how correct this model ultimately proves to be, the data presented here raise a number of important questions that are not directly addressed by the model. For example, why does IQGAP1 bind to cortical MFs, but is excluded from stress fibers? A potentially very complex issue concerns calmodulin. Each IQGAP1 molecule contains four calmodulin-binding IQ motifs per 190K subunit, or eight sites altogether. Depending upon exactly which sites are occupied by calmodulin at a given moment, as many as 256 different states of IQGAP1 may exist with respect to calmodulin binding. How, then, are the properties of IQGAP1 influenced by the number and locations of its bound calmodulins? Are all of the calmodulin sites involved in regulating MF binding, or do they control additional properties of IQGAP1, such as binding to Cdc42 or Rac? Another intriguing issue is whether IQGAP1 interacts with molecules other than Cdc42, Rac, calmodulin, and actin. Consistent with this possibility is the finding that IQGAP1 contains a WW domain (17), a recently recognized motif which is characterized by a pair of conserved tryptophan residues (39) and has been proposed to interact with serine-threonine protein kinases (14). The evidence presently available supports the hypothesis that IQGAP1 lies in the midst of a complex signal transduction network that regulates cortical MF organization. The stage has now been set for defining the specific functions and mechanisms of IQGAP1 within that network.

We thank Dr. William J. Snell for his advice throughout this study, for reviewing the manuscript, and for assistance with the EM; Valerie Nicolas for assistance with the EM; Dr. Jeffrey D. Jones for providing G-actin; Dr. Clive Slaughter and Caroline Moomaw for performing the peptide microsequencing; Dr. Joseph Albanesi for advice about falling ball viscometry and Scatchard analysis; Dr. Samuel Chacko for providing calmodulin; and Dr. Jean-Marie Sontag for sharing his keen insights with us during the latter stages of this project, and for reviewing the manuscript.

This work partially fulfills the Ph.D. requirements for A.-M. Bashour, and was supported by grants to G.S. Bloom from the National Institutes of Health (NS30485), the Robert A. Welch Foundation (I-1236), and the American Cancer Society (CB-58E).

Received for publication 9 January 1997 and in revised form 25 April 1997.

References

- Amano, M., K. Chihara, K. Kimura, Y. Fukata, N. Nakamura, Y. Matsumura, and K. Kaibuchi. 1997. Formation of actin stress fibers and focal adhesions enhanced by Rho-kinase. *Science (Wash. DC)*. 275:1308–1311.
- Andre, E., F. Lottspeich, M. Schleicher, and A. Noegel. 1988. Severin, gelsolin, and villin share a homologous sequence in regions presumed to contain F-actin severing domains. *J. Biol. Chem.* 263:722–727.
- Bagrodia, S., B. Derijard, R.J. Davis, and R.A. Cerione. 1995. Cdc42 and PAK-mediated signaling leads to Jun kinase and p38 mitogen-activated protein kinase activation. *J. Biol. Chem.* 270:27995–27998.

- Blanchard, A., V. Ohanian, and D. Critchley. 1989. The structure and function of alpha-actinin. *J. Muscle Res. Cell Motil.* 10:280–289.
- Bloom, G.S., M.C. Wagner, K.K. Pfister, and S.T. Brady. 1988. Native structure and physical properties of bovine brain kinesin and identification of the ATP-binding subunit polypeptide. *Biochemistry.* 27:3409–3416.
- Blum, H., H. Beier, and H.J. Gross. 1987. Improved silver staining of plant proteins, RNA and DNA in polyacrylamide gels. *Electrophoresis.* 8:93–99.
- Bretscher, A., and K. Weber. 1980. Fimbrin, a new microfilament-associated protein present in microvilli and other cell surface structures. *J. Cell Biol.* 86:335–340.
- Brill, S., S. Li, C.W. Lyman, D.M. Church, J.J. Wasmuth, L. Weissbach, A. Bernards, and A. Snijders. 1996. The Ras GTPase-activating-protein-related human protein IQGAP2 harbors a potential actin binding domain and interacts with calmodulin and Rho family GTPases. *Mol. Cell Biol.* 16:4869–4878.
- Cantor, C.R., and P.R. Schimmel. 1980. *Biophysical Chemistry*. W.H. Freeman and Co., New York. 1371 pp.
- Condeelis, J. 1993. Life at the leading edge: the formation of cell protrusions. *Annu. Rev. Cell Biol.* 9:411–444.
- Conrad, P.A., E.J. Smart, Y.-S. Ying, R.G.W. Anderson, and G.S. Bloom. 1995. Caveolin cycles between plasma membrane caveolae and the Golgi complex by microtubule-dependent and microtubule-independent steps. *J. Cell Biol.* 131:1421–1433.
- Coso, O.A., M. Chiariello, J.C. Yu, H. Teramoto, P. Crespo, N. Xu, T. Miki, and J.S. Gutkind. 1995. The small GTP-binding proteins Rac1 and Cdc42 regulate the activity of the JNK/SAPK signaling pathway. *Cell.* 81:1137–1146.
- Dedman, J.R., and M.A. Kaetzel. 1983. Calmodulin purification and fluorescent labeling. *Methods Enzymol.* 102:1–8.
- Einbond, A., and M. Sudol. 1996. Toward prediction of cognate complexes between the WW domain and proline-rich ligands. *FEBS (Fed. Eur. Biochem. Soc.) Lett.* 384:1–8.
- Fechheimer, M., and S.H. Zigmond. 1983. Changes in cytoskeletal proteins of polymorphonuclear leukocytes induced by chemotactic peptides. *Cell Motil.* 3:349–361.
- Gotlieb, A.I., and W. Spector. 1981. Migration into an in vitro experimental wound: a comparison of porcine aortic endothelial and smooth muscle cells and the effect of culture irradiation. *Am. J. Pathol.* 103:271–282.
- Hart, M.J., M.G. Callow, B. Souza, and P. Polakis. 1996. IQGAP1, a calmodulin-binding protein with a RasGAP-related domain, is a potential effector for Cdc42Hs. *EMBO (Eur. Mol. Biol. Organ.) J.* 15:2997–3005.
- Hartwig, J., J. Tyler, and T. Stossel. 1980. Actin-binding protein promotes the bipolar and perpendicular branching of actin filaments. *J. Cell Biol.* 87:841–848.
- Joneson, T., M. McDonough, D. Bar-Sagi, and L. Van Aelst. 1996. RAC regulation of actin polymerization and proliferation by a pathway distinct from Jun kinase. *Science (Wash. DC)*. 274:1374–1376.
- Kozma, R., S. Ahmed, A. Best, and L. Lim. 1995. The Ras-related protein, Cdc42Hs, and bradykinin promote formation of peripheral actin microspikes and filopodia in Swiss 3T3 fibroblasts. *Mol. Cell Biol.* 15:1942–1952.
- Kuroda, S., M. Fukata, K. Kobayashi, M. Nakafuku, N. Nomura, A. Iwamatsu, and K. Kaibuchi. 1996. Identification of IQGAP as a putative target for the small GTPases, Cdc42 and Rac1. *J. Biol. Chem.* 271:23363–23367.
- Kwiatkowski, D.J., T.P. Stossel, S.H. Orkin, J.E. Mole, H.R. Colten, and H.L. Yin. 1986. Plasma and cytoplasmic gelsolins are encoded by a single gene and contain a duplicated actin-binding domain. *Nature (Lond.)*. 323:455–458.
- Laemmli, U.K. 1970. Cleavage of structural proteins during the assembly of the head of bacteriophage T4. *Nature (Lond.)*. 227:680–685.
- Lamarche, N., N. Tapon, L. Stowers, P.D. Burbelo, P. Aspenstrom, T. Bridges, J. Chant, and A. Hall. 1996. Rac and Cdc42 induce actin polymerization and G1 cell cycle progression independently of p65^{PAK} and the JNK/SAPK MAP kinase cascade. *Cell.* 87:519–529.
- McCallum, S.J., W.J. Wu, and R.A. Cerione. 1996. Identification of a putative effector of Cdc42Hs with high sequence similarity to the RasGAP-related protein IQGAP1 and a Cdc42Hs binding partner with similarity to IQGAP2. *J. Biol. Chem.* 271:21732–21737.
- Minden, A., A. Lin, F.X. Claret, A. Abo, and M. Karin. 1995. Selective activation of the JNK signaling cascade and c-Jun transcriptional activity by the small GTPases Rac and Cdc42Hs. *Cell.* 81:1147–1157.
- Nobes, C.D., and A. Hall. 1995. Rho, Rac, and Cdc42 GTPases regulate the assembly of multimolecular focal complexes associated with actin stress fibers, lamellipodia and filopodia. *Cell.* 81:53–62.
- Olson, M.F., A. Ashworth, and A. Hall. 1995. An essential role for Rho, Rac and Cdc42 GTPases in cell cycle progression through G1. *Science (Wash. DC)*. 269:1270–1272.
- Onoda, K., and H.L. Yin. 1993. gCap39 is phosphorylated. Stimulation by okadaic acid and preferential association with nuclei. *J. Biol. Chem.* 268:4106–4112.
- Pardee, J.D., and A.J. Spudich. 1982. Purification of muscle actin. *Methods Enzymol.* 85:164–181.
- Pollard, T.D., and J.A. Cooper. 1982. Methods to characterize actin fila-

- ment networks. *Methods Enzymol.* 85:211–233.
32. Pollet, R.J. 1985. Characterization of macromolecules by sedimentation equilibrium in the air-turbine ultracentrifuge. *Methods Enzymol.* 117:3–27.
 33. Ridley, A.J., and A. Hall. 1992. The small GTP-binding protein rho regulates the assembly of focal adhesions and actin stress fibers in response to growth factors. *Cell.* 70:389–399.
 34. Ridley, A.J., H.F. Paterson, C.L. Johnston, D. Diekman, and A. Hall. 1992. The small GTP-binding protein rac regulates growth factor-induced membrane ruffling. *Cell.* 70:401–410.
 35. Sacks, D.B., S.E. Porter, J.H. Ladenson, and J.M. McDonald. 1991. Monoclonal antibody to calmodulin: development, characterization, and comparison with polyclonal anti-calmodulin antibodies. *Anal. Biochem.* 194: 369–377.
 36. Salisbury, J.L., A.T. Baron, and M.A. Sanders. 1988. The centrin-based cytoskeleton of *Chlamydomonas reinhardtii*: distribution in interphase and mitotic cells. *J. Cell Biol.* 107:635–641.
 37. Sellers, J.R., and H.V. Goodson. 1995. Motor proteins 2: myosin. *Protein Profile.* 2:1323–1423.
 38. Sheterline, P., J. Clayton, and J. Sparrow. 1995. Actin. *Protein Profile.* 2:1–103.
 39. Sudol, M., H.I. Chen, C. Bougeret, A. Einbond, and P. Bork. 1995. Characterization of a novel protein-binding module—the WW domain. *FEBS (Fed. Eur. Biochem. Soc.) Lett.* 369:67–71.
 40. Weissbach, L., J. Settleman, M.F. Kalady, A.J. Snijders, A.E. Murthy, Y.-X. Yan, and A. Bernards. 1994. Identification of a human rasGAP-related protein containing calmodulin-binding domains. *J. Biol. Chem.* 269: 20517–20521.
 41. Wolenski, J.S. 1995. Regulation of calmodulin-binding myosins. *Trends Cell Biol.* 5:310–316.
 42. Zhang, S., J. Han, M.A. Sells, J. Chernoff, U.G. Knaus, R.J. Ulevitch, and G.M. Bokoch. 1995. Rho family GTPases regulate p38 mitogen-activated protein kinase through the downstream mediator Pak1. *J. Biol. Chem.* 270:23934–23936.